

## 5.2 Results for Non-Separating Conditions

### 5.2.1 Determination of Mixing Section Inlet Conditions

To study the problem of recirculation, a new mixing section with a smaller diameter was built and tested (Fig. 5.2). A smaller diameter would increase the Hill number (Eqn. 5.1) and thus reduce the tendency toward recirculation. The new section is also straight, since having a diffuser in the earlier section proved to be another source for recirculation. Despite these constraints, it was still desired to have a diameter large enough so that flow conditions could be changed to trip the flow into separation. By having conditions with and without recirculation, this phenomenon could be studied more completely.

The code was tested against data from the new section for one run. Table 5.1 shows the conditions prevailing at the inlet to the section. Since the objective here is to analyze flow in the mixing section, exit conditions of the motive and suction nozzles must be provided. As discussed earlier, the code in its present state cannot compute the flow in the motive nozzle, so this information instead comes from Harrell's one-dimensional slip flow model.

This model is a combination of the motive nozzle flow regime transition shock (FRTS) and empirical pressure rise data in the mixing section. Harrell essentially asks what velocity of liquid and vapor is required at the motive nozzle outlet to provide the pressure rise seen experimentally in the mixing section. He guesses a liquid velocity for the outlet of the motive nozzle and then assumes that an FRTS occurs where the HEM velocity of the flow reaches the guessed liquid velocity. At this point the liquid continues toward the exit at a constant velocity while the vapor slows down as it traverses the diverging remainder of the motive nozzle subsonically. Thus, the vapor velocity at the outlet of the

nozzle can be found. Now, using a momentum balance on the mixing section the pressure rise can be found. If it is the same as what was seen experimentally, the initial liquid velocity guess is assumed to be good. Somewhat surprisingly, a high value of slip is required to match the mixing section pressure rise. As noted in Table 5.1 it is equal to 0.39 (motive vapor velocity/motive liquid velocity) for the one case that was considered.

Table 5.1 - Flow Conditions for Non-Recirculating Ejector		
Item	Dimensional	Nondim.
Motive Liquid Velocity	275 ft/sec (83.82 m/sec)	1
Motive Vapor Velocity	107 ft/sec (32.61 m/sec)	0.39
Motive Flow Quality	.026	
Suction Vapor Velocity	142.7 ft/sec (43.49 m/sec)	0.52
Density of Vapor	1.5 lbm/ft <sup>3</sup> (24.03 kg/m <sup>3</sup> )	0.019
Density of Liquid	77.5 lbm/ft <sup>3</sup> (1241.45 kg/m <sup>3</sup> )	
Viscosity of Vapor	0.0283 lbm/ft-h (.0421 kg/m-h)	0.049
Viscosity of Liquid	0.5724 lbm/ft-h (.8518 kg/m-h)	1
Reynold's Number (for nondim. eqns.)	3,500,000	
Motive Nozzle Outlet Radius	0.225 in. (.572 cm)	0.72
Mixing Section Radius	5/16 in. (.794 cm)	1
Initial Droplet Diameter	0.00125 in. (.00318 cm)	0.004
Inner Wall Turbulence Constants	$A = 26$ (dimensionless)	$\kappa = .6$
Jet/Outer Wall Turbulence Constant	$\kappa_o = .12$ (dimensionless)	$Co = .12$

## 5.2.2 Results for Mixing Section Pressure Rise

Figure 5.3 shows the resulting experimental pressure rise compared to the rise obtained with the code. Although the code predicts the pressure profile well, it is necessary to explain what adjustments were made to obtain this result. Two constants, the droplet diameter and  $\kappa_0$  (see Eqn. 3.16) were varied until the profile matched the experimental data. It should be noted that several of the standard equations for finding droplet diameter yield much different results, so it is not known with any certainty what the true diameter is. The most common approach, the use of Weber number, as shown in Eqn. 3.11 gives an initial droplet diameter for this flow about twenty times smaller than what was actually used. More is known about the jet mixing length constant,  $\kappa_0$ . This value in single phase flow is frequently taken to be around .08 (see Schetz [51]). For this problem, a value of .12 was used. The justification for this increase lies in the greater turbulence induced by the two-phase mixing, although no quantitative method was used to predict this.

The pressure rise for several other droplet diameters and jet mixing turbulence constants is given in Figures 5.4 and 5.5. These graphs show that the droplet diameter primarily influences the rate and amount of pressure rise at the beginning of the duct, whereas the turbulence constant affects the rise toward the middle and end of the duct. This trend is explained by noting that since interfacial drag is greatest when the velocity difference of the liquid and vapor is greatest, its effect would occur at the beginning of the mixing section. The turbulence level, however, is influenced also by the thickness of the jet mixing zone, which increases further downstream.

Figure 5.6 shows velocity profiles of the liquid and vapor at various axial positions for this case. Also, Figures 5.7, 5.8, and 5.9 show a contour plot of the velocity profiles and the void fraction profile. The assumed flat profiles at the inlet to the flow change rapidly

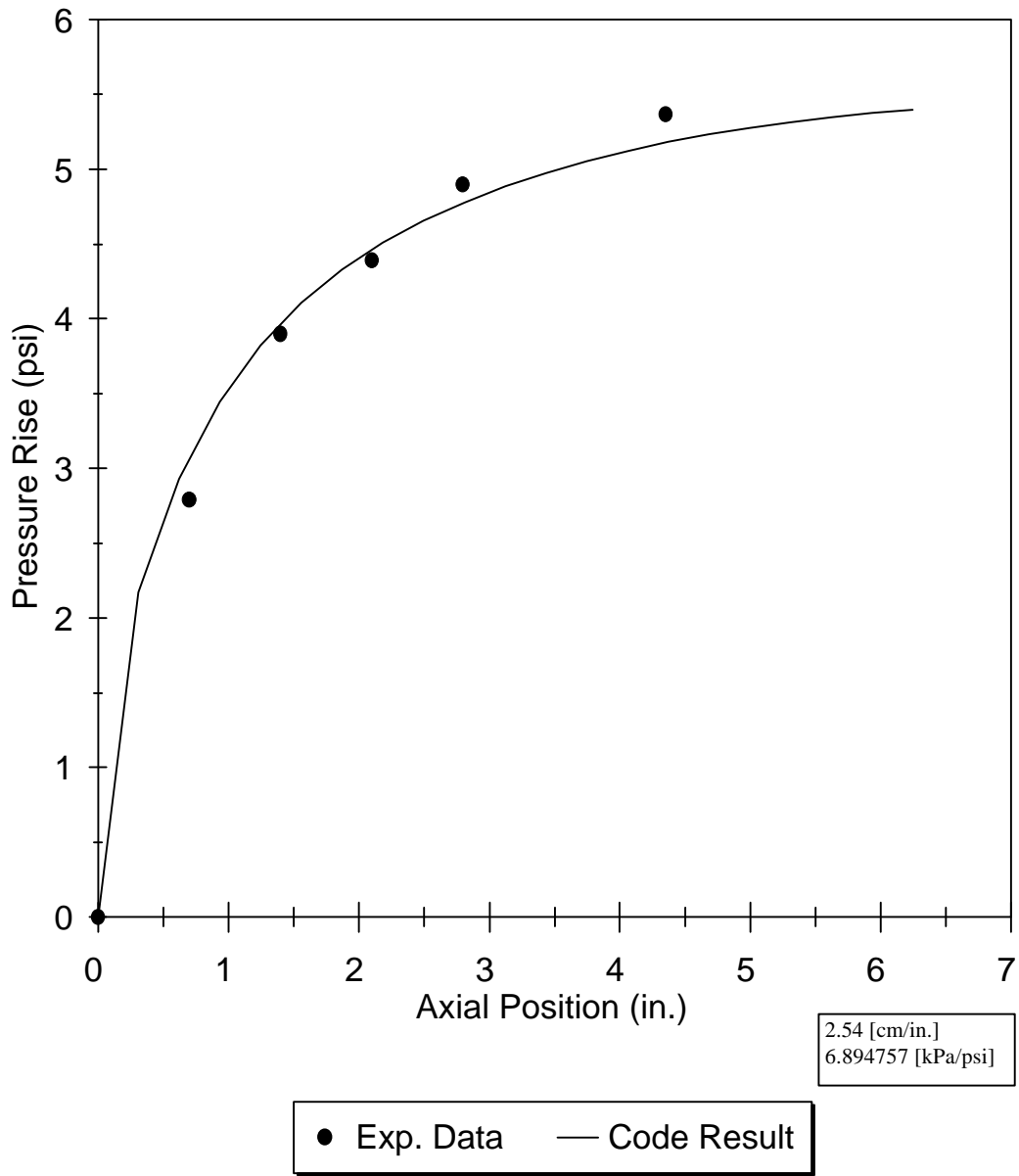
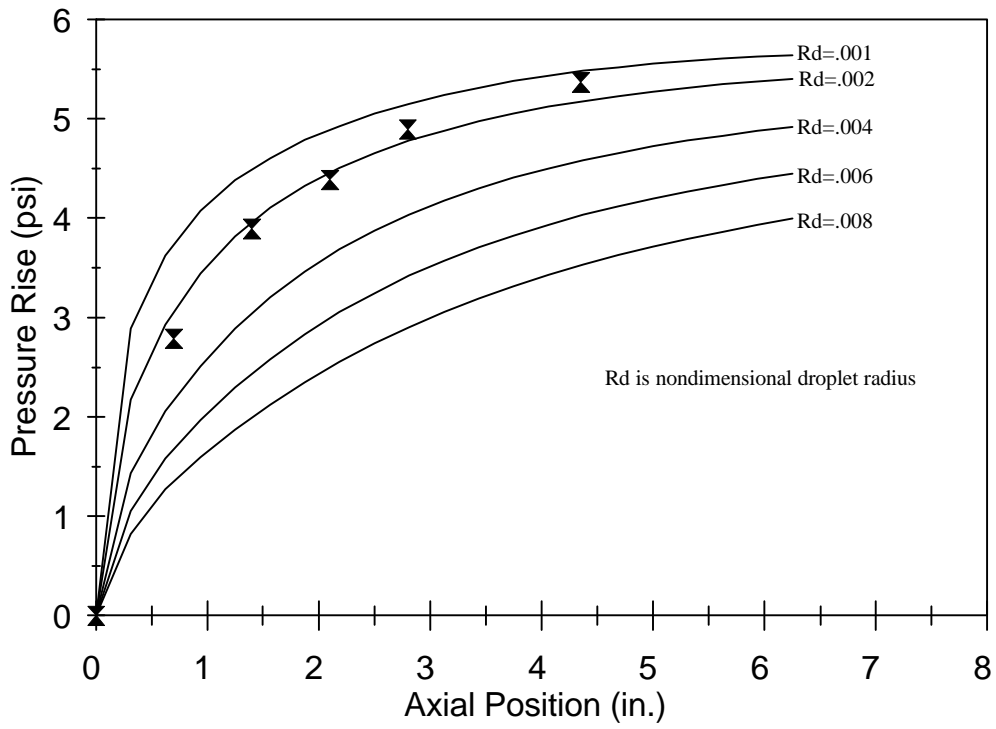


Figure 5.3 - Comparison of Experimental Pressure Rise and Code Results



2.54 [cm/in.]  
6.894757 [kPa/psi]

▲ Exp. Data

Figure 5.4 - Effect of Droplet Diameter on Pressure Rise

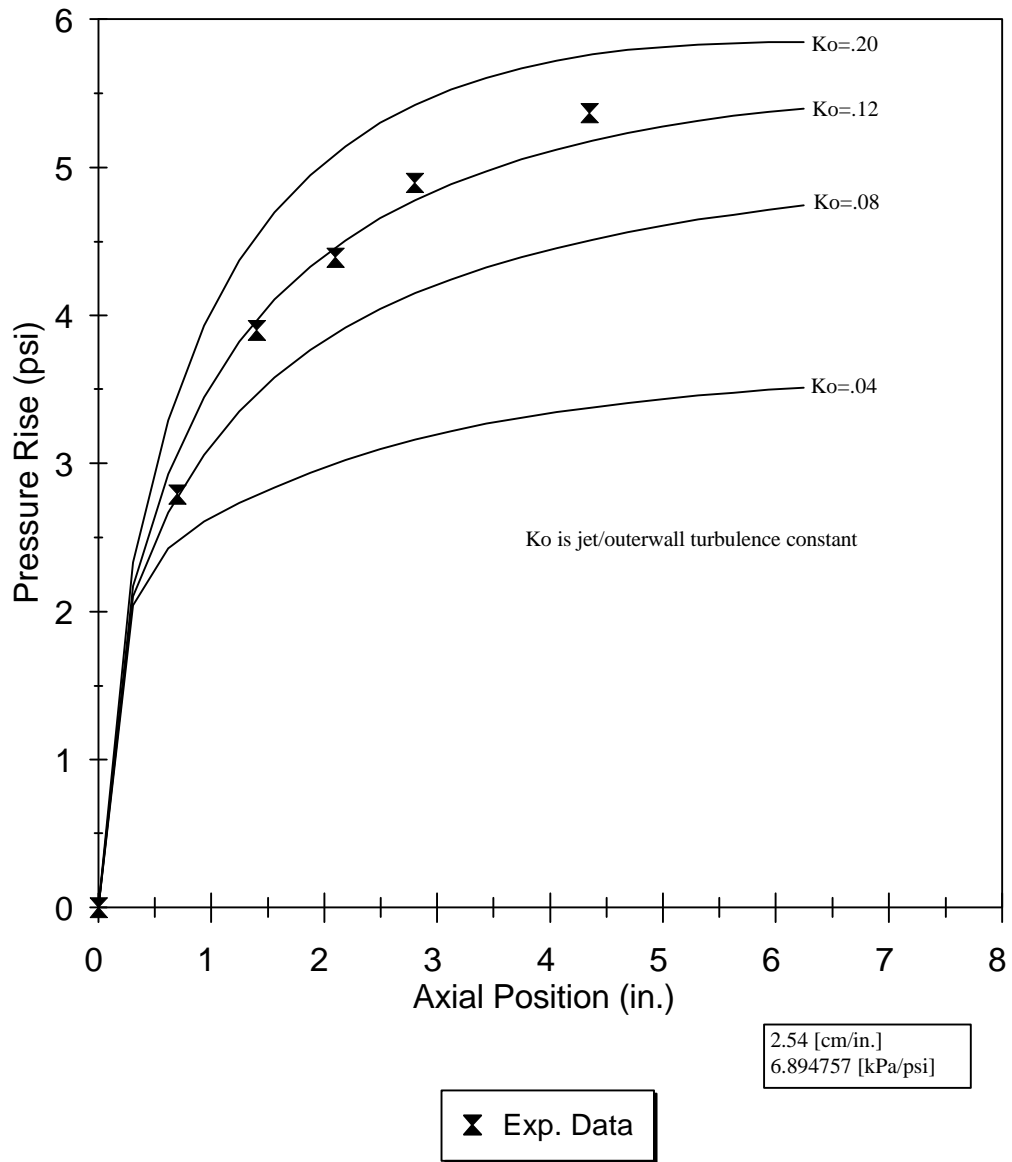


Figure 5.5 - Effect of Jet/Outerwall Turbulence Constant on Pressure Rise